Molecular Cell
Article

The Unstructured C-Terminal Tail of the 9-1-1 Clamp Subunit Ddc1 Activates Mec1/ATR via Two Distinct Mechanisms

Vasundhara M. Navadgi-Patil[1] and Peter M. Burgers[1,*]
[1]Department of Biochemistry and Molecular Biophysics, Washington University School of Medicine, St. Louis, MO 63110, USA
*Correspondence: burgers@biochem.wustl.edu
DOI 10.1016/j.molcel.2009.10.014

SUMMARY

DNA damage checkpoint pathways operate to prevent cell-cycle progression in response to DNA damage and replication stress. In *S. cerevisiae*, Mec1-Ddc2 (human ATR-ATRIP) is the principal checkpoint protein kinase. Biochemical studies have identified two factors, the 9-1-1 checkpoint clamp and the Dpb11/TopBP1 replication protein, as potential activators of Mec1/ATR. Here, we show that G1 phase checkpoint activation of Mec1 is achieved by the Ddc1 subunit of 9-1-1, while Dpb11 is dispensable. However, in G2, 9-1-1 activates Mec1 by two distinct mechanisms. One mechanism involves direct activation of Mec1 by Ddc1, while the second proceeds by Dpb11 recruitment mediated through Ddc1 T602 phosphorylation. Two aromatic residues, W352 and W544, localized to two widely separated, conserved motifs of Ddc1, are essential for Mec1 activation in vitro and checkpoint function in G1. Remarkably, small peptides that fuse the two tryptophan-containing motifs together are proficient in activating Mec1.

INTRODUCTION

Eukaryotic cells have evolved various repair mechanisms to deal with a wide range of genotoxic stresses. In addition to the DNA repair machinery, cells also possess vital checkpoint mechanisms that slow down cell-cycle progression and promote efficient repair to ensure genome integrity. In budding yeast *S. cerevisiae*, DNA checkpoints are activated by the PI3K-like protein kinase Mec1 (human ATR) and Tel1 (human ATM) (Bakkenist and Kastan, 2004; Harrison and Haber, 2006). While Tel1 specifically localizes to double-stranded DNA breaks, Mec1 is the principal PI3K kinase that initiates a signal transduction cascade in response to damage that leads to the generation of single-stranded DNA (ssDNA) coated with the ssDNA-binding protein RPA (Zou and Elledge, 2003). These include DNA damage processed by the nucleotide excision repair (NER) machinery in the G1 and G2 phases of the cell cycle, stalled replication forks during S phase, and uncompleted DNA replication intermediates and DNA damage during S/G2 (Giannattasio et al., 2004; Tercero and Diffley, 2001). Mec1 associates with accessory factor Ddc2 (human ATRIP) to form a heterodimeric Mec1-Ddc2 complex (Majka et al., 2006b). Ddc2 regulates the association of Mec1 with DNA (Rouse and Jackson, 2002; Zou and Elledge, 2003).

Along with Mec1, other sensor proteins and activators localize to sites of damage or stalled forks and participate in checkpoint activation. The 9-1-1 checkpoint clamp is a heterotrimer of the *S. cerevisiae* Ddc1, Rad17, and Mec3 proteins, the orthologs of *S. pombe*, and vertebrate Rad9, Hus1, and Rad1, respectively, hence the designation 9-1-1 (Parrilla-Castellar et al., 2004). Recent crystal structures of human 9-1-1 demonstrate a strong structural relationship of these subunits with the replication clamp PCNA (Doré et al., 2009; Sohn and Cho, 2009). The Rad24-RFC clamp loader for 9-1-1 differs from that of PCNA loader RFC, in that the Rad24 protein (*S. pombe* and human Rad17) replaces the Rfc1 subunit in a heteropentameric complex with the Rfc2–5 subunits (Green et al., 2000). The RFC and Rad24-RFC clamp loaders are very specific in loading PCNA and 9-1-1, respectively, and cannot substitute for each other (Majka and Burgers, 2003). RFC loads PCNA specifically onto 3′-primer/template junctions, where it can serve as a processivity factor for DNA polymerases. On the other hand, Rad24-RFC loads 9-1-1 specifically onto 5′-primer/template junctions (Majka et al., 2006a). This strict polarity of loading, which is opposite to that of PCNA, is also the required polarity for initiation of 9-1-1-dependent checkpoint activation in a *Xenopus laevis* egg extract system (MacDougall et al., 2007). The *S. cerevisiae* 9-1-1 clamp directly activates Mec1 kinase activity in vitro; however, this activity has not been demonstrated with 9-1-1 from other organisms (Majka et al., 2006b).

A second activator of Mec1/ATR is the essential replication protein Dpb11, designated Cut5/Rad4 in *S. pombe* and TopBP1 in human. In vitro, yeast Dpb11 has been shown to activate the kinase activity of Mec1 (Mordes et al., 2008; Navadgi-Patil and Burgers, 2008), and vertebrate TopBP1 can activate ATR (Choi et al., 2007; Kumagai et al., 2006). However, when in the cell cycle and how these two activators, 9-1-1 and Dpb11/Cut5/TopBP1, function is still uncertain. In the *S. cerevisiae* G1 and G2 phases of the cell cycle, the 9-1-1 clamp is essential for Rad53 hyperphosphorylation, which is an indicator of checkpoint activation (Longhese et al., 1997; Pellicioli et al., 1999), whereas checkpoint activation in response to replication fork stalling seems to be dependent on multiple partially redundant checkpoint proteins, including Dpb11 (Araki et al., 1995;

Frei and Gasser, 2000; Wang and Elledge, 2002). However, in *S. pombe* and in vertebrate cells, a somewhat different viewpoint of ATR activation has emerged, that of a strict interdependency of the 9-1-1 and Cut5/TopBP1 activators (Marchetti et al., 2002). One proposed model in these organisms is that the phosphorylated 9-1-1 clamp recruits Cut5/TopBP1 to stalled replication forks and damaged DNA sites, and Cut5/TopBP1 subsequently activates ATR (Delacroix et al., 2007; Furuya et al., 2004). Biochemical and genetic interactions between budding yeast 9-1-1 and Dpb11 have also been demonstrated, and these two factors exhibit synergism in Mec1 activation in vitro (Navadgi-Patil and Burgers, 2008; Puddu et al., 2008; Wang and Elledge, 2002). The 9-1-1 clamp subunit Ddc1/Rad9 has a conserved serine/threonine phosphorylation site near the extreme C terminus, which is involved in the recruitment of Dpb11/Cut5/TopBP1 (Furuya et al., 2004; Puddu et al., 2008). Thus, while the recruitment of Dpb11/Cut5/TopBP1 by 9-1-1 to sites of damage/fork stalling is well understood and appears to be conserved in all eukaryotes, the actual mechanism of Mec1/ATR activation by 9-1-1 still remains to be investigated. In particular, it is not clear at what stages of the cell cycle these proteins activate Mec1 and whether they act independently or in synergy.

The *S. cerevisiae* Ddc1 protein is the critical subunit of the 9-1-1 checkpoint clamp that mediates activation of Mec1 kinase activity (Bonilla et al., 2008; Majka et al., 2006b). The PCNA-like domain maps to the N-terminal 385 aa of Ddc1 (Doré et al., 2009; Sohn and Cho, 2009). In addition, Ddc1/Rad9 has a poorly conserved unstructured C-terminal region of varying length. In the 612 aa Ddc1 subunit, this C-terminal tail is 227 aa in length (Figure 1A). In this study, we show that the C-terminal tail is involved in checkpoint activation through two distinct mechanisms. First, we have identified two motifs in Ddc1 that are essential for Mec1 activation, one in the PCNA-like domain and one near the C terminus of the unstructured tail. Mutation of a conserved tryptophan in either motif, W352 or W544, greatly reduces Mec1 activation in vitro, and the double mutant is defective for the G1 checkpoint. Second, we demonstrate that, in addition to these two activation motifs, a conserved serine/threonine phosphorylation site near the extreme C terminus of the tail is required for robust checkpoint activation in the G2 phase of the cell cycle through recruitment of Dpb11 function. The two motifs in Ddc1 that are essential for activation of Mec1 are widely separated by nonconserved sequences. We show that these two motifs suffice for Mec1 activation by combining them in a single oligopeptide with biochemical activity.

RESULTS

The C-Terminal Tail of Ddc1 Is Required for Mec1 Activation In Vitro

Based on the recent crystal structures of the human 9-1-1 complex, the C-terminal tail of Ddc1 is estimated to be ~230 aa in length, and several secondary structure prediction programs assign a high degree of structural disorder to this tail (Figure 1A). We first generated a tailless form of Ddc1 (*ddc1-404*) that, based upon structural considerations, should keep the ability of Ddc1 to form a 9-1-1 clamp intact (Figure 1A). The analysis of this mutant is shown in Figure 1, as an example of the type of analysis carried out with additional mutants discussed later.

Overexpression in yeast of GST-*ddc1-404* together with *RAD17* and *MEC3* allowed us to purify heterotrimeric 9_{404}-1-1 by glutathione affinity chromatography, analogous to wild-type 9-1-1 (Majka and Burgers, 2003). After proteolytic cleavage of the GST tag, 9_{404}-1-1 was further purified as a 1:1:1 complex, confirming that the subunit interactions were not compromised in the mutant (Figure 1B). We next determined that the mutant clamp could be loaded onto DNA by its loader Rad24-RFC, and this loading required ATP (Majka and Burgers, 2003). The assay depends on our ability to separate free proteins from DNA-bound protein by size-exclusion chromatography, followed by analysis of the DNA-protein fraction by a western blot with Ddc1 antibodies. This analysis showed that the 9_{404}-1-1 clamp was loaded onto DNA in an ATP-dependent reaction, and this loading was as efficient as that of wild-type 9-1-1 (Figure 1C).

Having established that clamp subunit interactions and loading were not impaired by deletion of the Ddc1 C-terminal tail, we next tested the mutant in a checkpoint activation system. This consists of primed single-stranded effector DNA coated with the single-stranded binding protein RPA, wild-type or mutant 9-1-1 clamp, the Rad24-RFC clamp loader, the heterodimeric kinase Mec1-Ddc2 (hereafter simply referred to as Mec1), and a kinase-dead version of Rad53 (Rad53-kd = Rad53-K227A) as a physiological target to record activation of Mec1 (Figure 1D). The kinase-dead mutant of Rad53 was used in these studies to ensure that all observed phosphorylation events were Mec1 dependent. Previous studies have shown that activated Mec1 phosphorylates the Rpa1 and Rpa2 subunits of RPA, the Rad24 subunit of the clamp loader, the checkpoint clamp subunits Ddc1 and Mec3, and Rad53; these same targets are also phosphorylated in vivo in response to genotoxic stress (discussed in Majka et al., 2006b). Mec1-mediated phosphorylation was followed with time. Wild-type 9-1-1 activated the basal activity of Mec1 ~20-fold. In comparison, the tailless 9_{404}-1-1 clamp was inactive. Significantly, the phosphorylation of all targets was increased in the presence of 9-1-1, and none was increased in the presence of 9_{404}-1-1, indicating that activation of Mec1 by 9-1-1 is global and not directed toward specific targets. These data show that at least one motif in the unstructured tail is required for Mec1 activation in vitro.

We also generated Ddc1 mutants with smaller C-terminal truncations, 1–508 aa and 1–562 aa (Figure S1). Both mutants formed checkpoint clamps with Rad17 and Mec3. These mutants were tested for their ability to activate Mec1 kinase activity in vitro. Similar to the 9_{404}-1-1 clamp, 9_{508}-1-1 was defective in activating Mec1 kinase at all concentrations tested (Figure S1C). However, the 9_{562}-1-1 clamp was proficient in activating Mec1, suggesting that a sequence within Ddc1 residues 508–562 is critical for activation.

The C-Terminal Tail of Ddc1 Is Required for G1 Checkpoint Activation

Next, we studied whether the tailless *ddc1-404* mutant could complement the damage sensitivity and checkpoint defects of a *ddc1Δ* strain. Checkpoint activation in the G1 phase of the

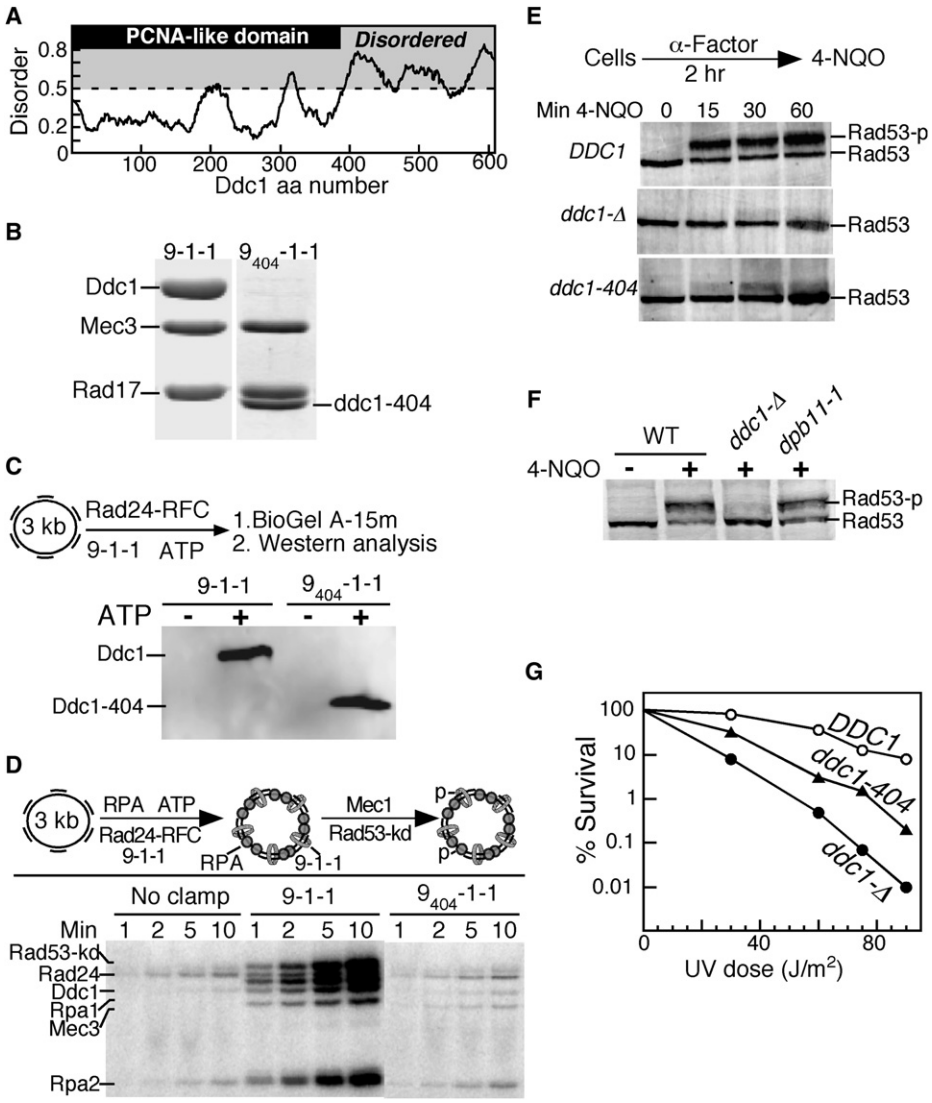

Figure 1. The Ddc1 C-Terminal Tail Is Involved in the Activation of Mec1 Kinase in the G1 Phase

(A) Domain map of Ddc1. The PCNA-like domain (1–385 aa) is indicated in gray. Disordered regions were obtained by submitting the Ddc1 sequence to disorder-prediction programs (IUPRED [http://iupred.enzim.hu], PONDR [http://www.pondr.com], and PrDOS [http://prdos.hgc.jp]) and averaging the output. A disorder value >0.5 is considered to indicate an unstructured protein region.

(B) Coomassie-stained 10% SDS-PAGE gel showing the copurification of Rad17 and Mec3 with wild-type Ddc1 or with Ddc1-404 after overexpression in yeast. The migration position of clamp subunits is indicated.

(C) The PCNA-like domain of Ddc1 is sufficient to form a 9-1-1 clamp that can be loaded onto DNA by Rad24-RFC in an ATP-dependent manner. The loaded clamp is detected by western analysis with anti-Ddc1 antibodies. A flow diagram of the loading assay is shown. See Experimental Procedures for details.

(D) A flow diagram of the complete in vitro phosphorylation assay as described in Experimental Procedures is shown. Aliquots were taken at the indicated times and analyzed by SDS-PAGE.

(E) Western analysis of Rad53 phosphorylation in G1 cells. Wild-type, *ddc1Δ*, and *ddc1-404* cells were arrested in G1 phase and treated with 4NQO for the indicated times, as described in Experimental Procedures. The hyperphosphorylated form of Rad53 is indicated as Rad53-p.

(F) Strains were grown at 25°C, arrested in G1, and exposed to 4NQO for 60 min where indicated. A western analysis with Rad53 antibodies was performed.

(G) Dose-response survival curves of the indicated *DDC1* mutants (see Experimental Procedures for details).

yeast cell cycle is completely dependent on the 9-1-1 clamp (Pellicioli et al., 1999). Cells were first arrested in G1 phase with α mating factor and then treated with the UV-mimetic drug 4NQO (4-Nitroquinoline 1-Oxide). Phosphorylation of the effector kinase Rad53 was monitored by western analysis. In cells expressing wild-type *DDC1*, robust Rad53 hyperphosphorylation was already observed after 15 min, and this phosphorylation showed a further increase up to 1 hr of treatment with 4NQO (Figure 1E). The *ddc1Δ* mutant was completely defective in activating Rad53, while *ddc1-404* showed detectable Rad53 phosphorylation only after prolonged treatment with 4NQO. Furthermore, an in situ assay has been developed that detects

activated Rad53 (Pellicioli et al., 1999). In this assay, 9_{404}-1-1 also shows a strong defect in Rad53 activation (Figure S2A). The *ddc1-404* mutant also showed a G1 checkpoint defect in response to treatment with methyl methanesulfonate (MMS) (Figure S2B).

However, in asynchronous cells, Rad53 phosphorylation in response to 4NQO was not reduced in either the *ddc1Δ* or the *ddc1-404* mutant (Figure S2C). This is in agreement with earlier work that showed 9-1-1 to be dispensable for Rad53 phosphorylation in asynchronous cells in response to MMS and hydroxyurea, suggesting the existence of redundant pathways for DNA damage checkpoint activation in other stages of the cell cycle (Pellicioli et al., 1999).

Dpb11-1, a mutant lacking the Dpb11 C-terminal tail, is defective in S phase checkpoint activation, and the truncated protein fails to activate Mec1 in vitro (Araki et al., 1995; Mordes et al., 2008; Navadgi-Patil and Burgers, 2008). Damage-induced Rad53 phosphorylation in G1-arrested *dpb11-1* cells was only slightly reduced compared to wild-type, indicating that Dpb11 plays a negligible role in the G1 checkpoint (Figure 1F). These results strongly suggest that direct activation of Mec1 by the 9-1-1 clamp is crucial for checkpoint activation in G1 phase, and this activation involves the C-terminal tail of Ddc1. Finally, defects in checkpoints are associated with damage sensitivity and, indeed, the *ddc1-404* mutant was sensitive to UV irradiation (Figure 1G). However, the truncation mutant was significantly less sensitive than *ddc1Δ*, suggesting either residual checkpoint activity of the tailless 9-1-1 clamp or the participation of 9-1-1 in other repair pathways.

Ddc1 has five putative Mec1 phosphorylation sites (S/TQ) (Figure S3A), and phosphorylation of Ddc1 in response to DNA damage requires Mec1 (Longhese et al., 1997). Phosphorylation of the C-proximal threonine of *S. pombe* and human Rad9, which is analogous to T602 in Ddc1, is a critical step in checkpoint activation, since this modification promotes binding of 9-1-1 to Cut5/TopBP1 (Delacroix et al., 2007; Furuya et al., 2004). We mutated either the single T602 residue (*ddc1-T602A*) or all five putative serine/threonine residues, including T602, to alanine (*ddc1-5S/T5A*) and purified the mutant $9_{5S/T5A}$-1-1 clamp. This mutant clamp was fully proficient for loading onto DNA and efficiently activated Mec1 to phosphorylate RPA and Rad53 in our in vitro system (Figure S3A). Significantly, however, Mec1-mediated phosphorylation of the mutant Ddc1-5S/T5A subunit was completely abrogated. The *ddc1-5S/T5A* mutant showed no G1 checkpoint defect, suggesting that phosphorylation of Ddc1 is not critical to Mec1 activation in G1 (Figure S3B). The fact that G1 checkpoint activation in *ddc1-5S/T5A* is unperturbed provides further evidence that Dpb11 is dispensable for checkpoint activation in G1 cells. This result contrasts fundamentally with those obtained with G2-arrested cells, which will be discussed below.

A Motif in the PCNA-like Domain of Ddc1 Is Essential for Mec1 Activation

In order to gain a more precise understanding of the sequence and structural determinants in Ddc1 important for Mec1 activation, it became necessary to dissociate Ddc1's activation properties from those that comprise its functionality as a clamp. We have previously described an assay in which Ddc1 alone can activate Mec1, without the other 9-1-1 subunits or the Rad24-RFC clamp loader and without effector DNA (Majka et al., 2006b). While this biochemical bypass assay, which can only be carried out at very low salt ($\leq$40 mM NaCl), is not physiological in nature, it has an analogous counterpart in the cell. The artificial colocalization onto chromatin of Ddc1 and Ddc2 and thereby Mec1 leads to gratuitous checkpoint activation, even in *mec3Δ* mutants that lack the ability to make a 9-1-1 clamp (Bonilla et al., 2008). In our experimental strategy, we first set out to define the motifs and specific amino acids in Ddc1 that are critical for Mec1 activation using the biochemical bypass assay. Subsequently, specific Ddc1 mutations were designed that are proficient for 9-1-1 heterotrimeric clamp formation and for clamp loading onto DNA but defective for Mec1 activation, and those mutants were investigated both in vitro and in vivo.

A multiple sequence alignment of Ddc1 and its homologs was carried out to identify conserved residues that might be involved in Mec1 activation. While the PCNA-like domain is highly conserved in all eukaryotes, the C-terminal domain is very poorly conserved, even in the closely related species of the *Saccharomycetales* order shown in Figure 2A. The most highly conserved motif is around the C-terminal phosphorylation site T612 that we showed above to be of minimal importance in Mec1 activation (Figure S3A). Since our analysis of the Ddc1-404 mutant showed that the Ddc1 C-terminal tail is required for Mec1 activation, we first generated Ddc1(405–612) to test if this tail was sufficient to activate Mec1 at low-salt conditions in vitro; however, it was not (Figure 2C), suggesting that additional N-proximal motif(s) were required. Therefore, we included larger N-terminal sequences. Ddc1(294–612) was similar to wild-type Ddc1 in activating Mec1, whereas Ddc1(340–562) showed only slightly reduced Mec1 activation (Figure 2C). Ddc1(348–562) still showed substantial activity, but a further 11 aa N-terminal truncation to Ddc1(357–562) resulted in a total loss of activity. These mapping studies suggest that, in addition to sequences in the unstructured tail, at least one motif toward the C-terminal end of the PCNA-like domain is also required for Mec1 activation. This region of the PCNA-like structure consists of two β strands connected by a loop and is highly conserved in eukaryotes (Figure S4). We mutated the conserved tripeptide motifs LWF351–353 in the first β strand and ILM360–362 in the second β strand to AAA, in the Ddc1(340–562) construct. When these mutants were tested for their ability to activate Mec1, the LWF → AAA mutant was totally defective in activating Mec1, whereas the ILM → AAA mutant still showed robust activity (Figure 2D).

In order to test these mutants in the complete, physiologically relevant biochemical assay that depends on the loading of 9-1-1 onto effector DNA substrate, the two triple mutants were generated into full-length Ddc1, and an attempt was made to isolate and purify intact mutant clamps. However, although the β strands of interest are distant from the subunit-subunit interfaces, neither mutant showed interactions with the Mec3 and Rad17 subunits of 9-1-1, suggesting that the mutant proteins were misfolded (Figures S5A and S5B). In support of that conclusion, the *ddc1-LWF351AAA* and *ddc1-ILM360AAA* mutants were as sensitive as the *ddc1Δ* strain to UV and camptothecin exposure

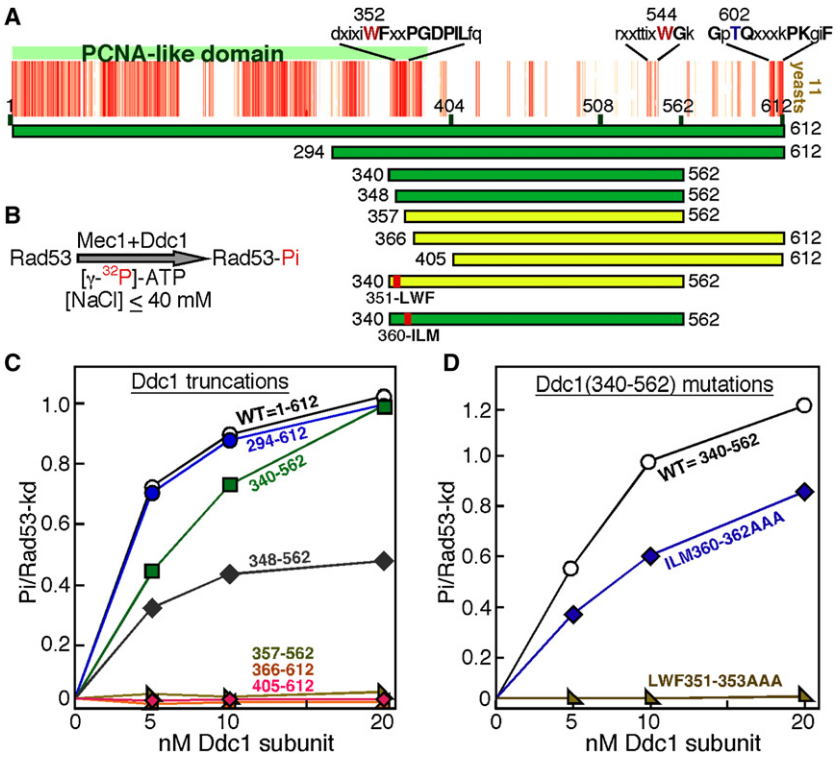

Figure 2. Mapping of a Mec1 Activation Determinant in the PCNA-like Domain of Ddc1

(A) Multiple sequence alignment of 11 Ddc1 species from the *Saccharomycetales* order (budding yeast; see also Figure S4) using Kalign with a gap penalty of 5 and a gap extension penalty of 0.5 (default is 11, 0.7). Each red bar indicates strong identity with the consensus, and each pink bar indicates conservation with the consensus. Note that the occurrence of multiple gaps has spread out the 404–612 region. The conserved motifs and aa of interest are indicated. Ddc1 domains tested for Mec1 activation in the low-NaCl bypass assay are shown with bars (green is active, yellow is inactive).

(B) Flow diagram of the bypass Mec1 activation assay by Ddc1 at 40 mM NaCl, used in (C) and (D). The bypass assay does not require a heterotrimeric 9-1-1 clamp, Rad24-RFC clamp loader, or DNA (see Experimental Procedures).

(C) Quantification of Rad53-kd phosphorylation by Mec1, activated by increasing levels of the Ddc1 domains shown in (A). Background phosphorylation of Rad53-kd by Mec1, obtained in the absence of Ddc1, was subtracted.

(D) Quantification of Rad53-kd phosphorylation by Mec1, activated by increasing levels of the Ddc1 (340–562) protein with triple point mutants as shown in (A).

and as defective as *ddc1Δ* for G1 checkpoint activation after 4NQO treatment (Figures S5C and S5D).

Focusing only on the first β strand, which showed a complete defect in Mec1 activation in the triple mutant (Figure 2D), we made the single W352A mutant, because it was the only amino acid in the LWF motif that was solvent-exposed and therefore unlikely to seriously affect folding. Ddc1-W352A was proficient in forming a checkpoint clamp with Rad17 and Mec3, and the mutant 9_{W352A}-1-1 clamp was loaded as efficiently as wild-type onto primed DNA by the Rad24-RFC clamp loader in an ATP-dependent manner (Figure 3A). However, the mutant clamp showed a ~20-fold reduction in Mec1 activation (Figure 3B).

Bipartite Mec1 Activation Determinants in Ddc1

In addition to W352, our analysis with the tailless Ddc1-404 mutant showed that determinants in the C-terminal tail are required for Mec1 activation. We carried out a comparative analysis of 11 species in the *Saccharomycetales* (budding yeasts) order (Figure 2A). The identification of small conserved motifs required that the gap penalty in the alignment program was set very low. Our interest focused on a very small motif around aa 540, because (1) this motif is contained in the 9_{562}-1-1 clamp proficient for Mec1 activation, but is lacking from the deficient 9_{508}-1-1 clamp (Figure S1C), and (2) it contains a relatively conserved tryptophan-glycine dipeptide motif (Figure S4). A mutant clamp was prepared with a Ddc1-W544A mutation. While the mutant 9_{W544A}-1-1 clamp was efficiently loaded onto DNA, it showed a ~10-fold decrease in Mec1 activation capacity (Figure 3B). We also made the double mutant, designated Ddc1-2W2A, combining both the W352A mutation in the PCNA-like domain and the W544A tail mutation. The double mutant efficiently formed the heterotrimeric 9_{2W2A}-1-1 clamp with Mec3 and Rad17 (data not shown) and was efficiently loaded onto effector DNA by Rad24-RFC in an ATP-dependent manner (Figure 3A); however, the loaded clamp was completely defective in the activation of Mec1 (Figure 3B). Therefore, two conserved tryptophan residues anchor the two motifs that are essential for Mec1 activation.

While the Ddc1-2W2A mutant completely abrogates Mec1 activation, it retains interactions with Dpb11. Previously, we described that the interactions between 9-1-1 and Dpb11 resulted in synergism in Mec1 activation (Navadgi-Patil and Burgers, 2008). Mutant 9_{2W2A}-1-1 stimulated the activation of Mec1 by Dpb11 3- to 4-fold, while the tailless mutant 9_{404}-1-1 did not (Figure S6). Together with the results of the phosphorylation-defective $9_{5S/T5A}$-1-1 mutant clamp (Figure S3), this indicates that we have separated the two functions of Ddc1: activation of Mec1 and recruitment of Dpb11.

The DNA Damage Checkpoint in G1 Predominantly Requires Mec1 Activation by 9-1-1

We next tested the phenotypes of the single W → A mutants and the double mutant in damage sensitivity and checkpoint functionality. Interestingly, the *ddc1-W544A* mutation, which was associated with a ~10-fold reduction in activation capacity in our biochemical assay, was only slightly impaired in Rad53 phosphorylation in G1 cells in response to DNA damage (Figure 3C). This result would suggest that full checkpoint activation in vivo can be accomplished even when the clamp is only partially active. In agreement with this idea, the *ddc1-W352A*

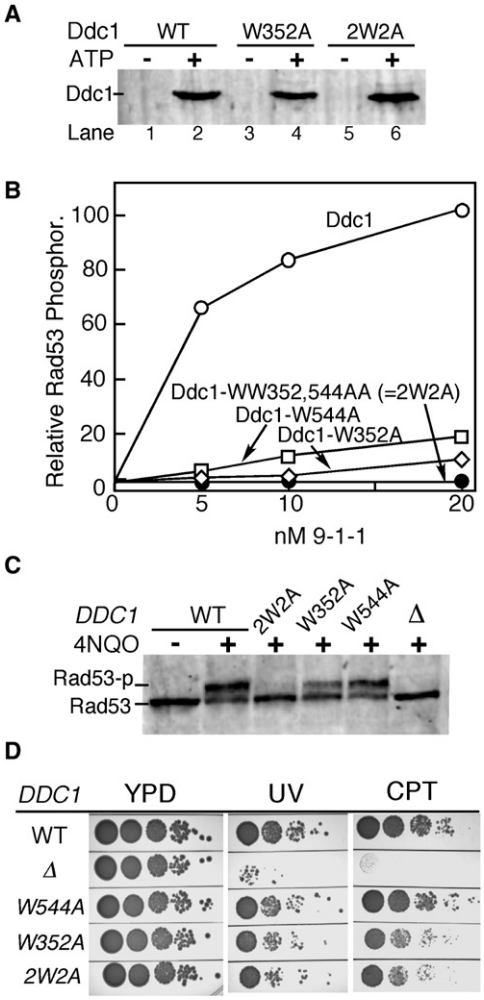

Figure 3. Mapping of Bipartite Mec1 Activation Motifs in Ddc1

(A) Ddc1-W352 and Ddc1-2W2A (WW352,544AA) form functional 9-1-1 clamps that can be loaded onto DNA by Rad24-RFC in an ATP-dependent manner. See legend to Figure 1C and Experimental Procedures for details.

(B) The complete in vitro Mec1 phosphorylation assay was carried out at 125 mM NaCl with indicated levels of (mutant) 9-1-1 clamps (see Figure 1D and Experimental Procedures for details). Phosphorylation of Rad53-kd is quantified. Background phosphorylation of Rad53-kd by Mec1, obtained in the absence of Ddc1, was subtracted.

(C) Western analysis of G1-arrested cells exposed to 4NQO for 30 min.

(D) Serial dilutions (10-fold) of wild-type cells and the indicated *DDC1* mutants were tested for sensitivity to UV (60 J/m^2) or camptothecin (10 μg/ml). Plates were incubated at 30°C for 2 days and photographed.

mutation, which is associated with a ~20-fold reduction in activation capacity in our biochemical assay, still showed significant albeit reduced Rad53 phosphorylation in G1 cells in response to DNA damage. It required the complete in vitro activation defect of the *ddc1-2W2A* double mutant in order to generate a defective checkpoint response in G1 cells in response to 4NQO treatment (Figures 3B and 3C).

Despite the complete G1 checkpoint defects of the double mutant, the strain was still much less sensitive to UV or camptothecin treatment than the *ddc1Δ* strain (Figure 3D). Unexpectedly, *ddc1-2W2A* was not more sensitive than the single *ddc1-W352A* mutant that still showed residual Mec1 activation in vitro (Figure 3). However, when checkpoint function was further sensitized by the additional *dpb11-1* mutation, *ddc1-2W2A* was more sensitive than *ddc1-W352A* to growth on hydroxyurea or camptothecin media (Figure S7). The moderate sensitivity of *ddc1-2W2A* to DNA damaging agents suggests the potential for additional checkpoint functionality of the 9_{2W2A}-1-1 clamp in other phases of the cell cycle, as described below for G2, and/or participation of the mutant clamp in other DNA damage response pathways.

A Robust G2 Checkpoint Requires Both the Activation Capacity of Ddc1 and Its Interaction with Dpb11

G2 phase checkpoint activation is dependent on the 9-1-1 clamp (Longhese et al., 1997), and a recent study shows that phosphorylation of Ddc1 is required in order to elicit a full G2 phase checkpoint (Puddu et al., 2008). However, these analyses have not addressed whether direct activation of Mec1 by Ddc1 is involved in the G2 checkpoint or whether activation proceeds solely via recruitment of Dpb11 by Ddc1. Here, we have studied Rad53 phosphorylation in cells arrested with nocodazole in the G2 phase of the cell cycle and then treated with the UV-mimetic agent 4NQO. Similarly to G1 phase cells, G2 phase-arrested cells showed a strong checkpoint response after treatment with 4NQO, and this response was completely abrogated in the *ddc1Δ* mutant (Figure 4A, lane 3).

We next studied the phenotypes of the *ddc1-2W2A* mutant that eliminates activation of Mec1 and of the *ddc1-T602A* mutant that eliminates interaction with Dpb11. Both mutants showed a reduction in Rad53 phosphorylation upon damage exposure, yet a significant response remained (lanes 4 and 5). However, the combined *ddc1-2W2A,T602A* mutant was almost completely defective for the G2 checkpoint (lane 6). These results suggest the existence of two distinct pathways. The first involves direct activation of Mec1 by 9-1-1 that is Dpb11 independent, and this is abrogated in the *ddc1-2W2A* mutant but not in the *ddc1-T602A* mutant. The second pathway proceeds via recruitment of Dpb11 by 9-1-1 through the phosphorylated Ddc1 subunit and subsequent Mec1 activation by Dpb11; this pathway is abrogated in the *ddc1-T602A* mutant (Puddu et al., 2008) but not in the *ddc1-2W2A* mutant (Figure S6).

To further test this model, we also studied Rad53 phosphorylation in G2-arrested, 4NQO-treated *dpb11-1* cells. The *dpb11-1* mutant lacks the Dpb11 C-terminal tail and fails to activate Mec1 (Mordes et al., 2008; Navadgi-Patil and Burgers, 2008). *Dpb11-1* mutant cells were proficient in Rad53 phosphorylation in G2 phase, although the response, like that in *ddc1-T602A* cells, was less robust than in wild-type cells (Figure 4B, lane 3). However, the *dpb11-1 ddc1-2W2A* double mutant was almost completely defective for Rad53 phosphorylation, indicating that both pathways were eliminated (lane 4). Residual Rad53 phosphorylation was observed in the *ddc1-2W2A,T602A* triple mutant and in the combined *dpb11-1 ddc1-2W2A* mutant but not in a *DDC1* deletion (Figure 4). This residual response may operate through clamp-Tel1 interactions (Giannattasio et al., 2002). Finally, damage sensitivity measurements of the mutants lend additional support to a model that direct activation by

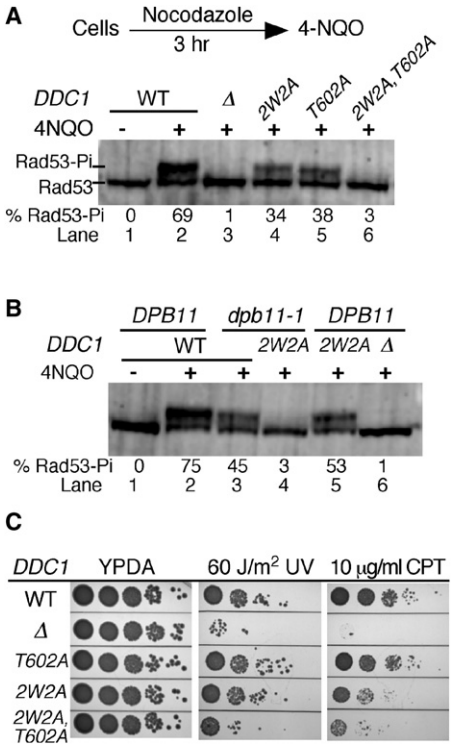

Figure 4. The 9-1-1 Clamp Activates Mec1 in G2 Cells via Two Distinct Mechanisms

(A) Log phase cells were arrested in G2 phase with nocodazole (20 μg/ml) for 3 hr at 30°C, then treated with 4NQO for 20 min. A western analysis of Rad53 phosphorylation was carried out as described in Experimental Procedures. The percent of hyperphosphorylated Rad53 is shown beneath the lanes.

(B) As in (A), except that the entire experiment was carried out at 23°C (*dpb11-1* is temperature sensitive for growth), nocodazole treatment was for 4 hr, and 4NQO treatment was for 20 min.

(C) Serial dilutions (10-fold) of wild-type cells and the indicated *DDC1* mutants were tested for sensitivity to UV (60 J/m^2) or camptothecin (10 μg/ml). Plates were incubated at 30°C for 2 days and photographed.

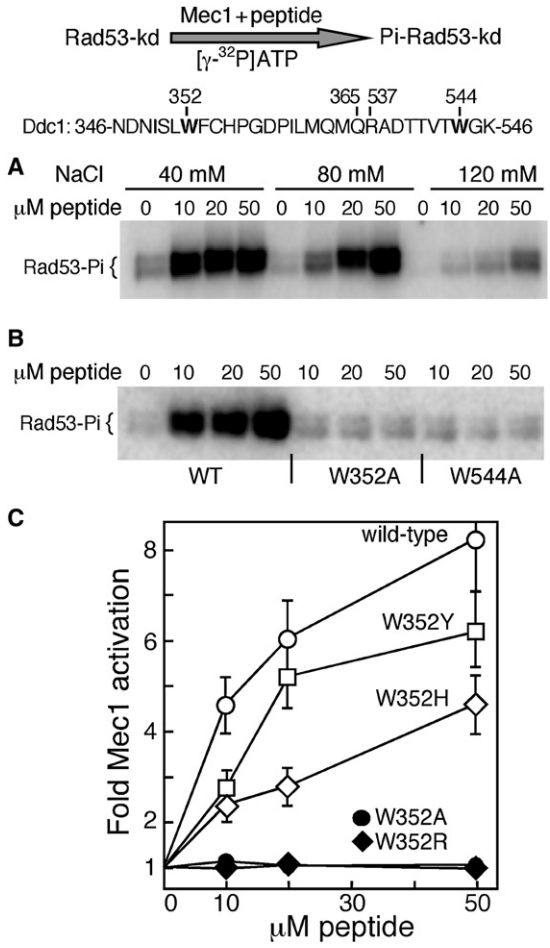

Figure 5. A Ddc1 Peptide Containing the Bipartite Mec1 Activation Sequence Activates Mec1

(A) A 30-mer peptide containing the bipartite Ddc1 sequence from 346 to 365 aa and from 537 to 546 aa is shown in (A)–(C). Residues W352 and W544 required for Mec1 activation are indicated. Shown in (A), kinase activity of Mec1 was detected using Rad53-kd as a substrate in buffer containing the indicated levels of NaCl. Increasing levels of Ddc1 peptide were added, and phosphorylated Rad53-kd was analyzed after 10 min.

(B) Ddc1 peptides with W352A or W544A mutations are inactive for Mec1 stimulation. The assay as in (A) was carried out in the presence of 60 mM NaCl.

(C) Quantification of Mec1 activation by Ddc1 peptides in (B), and those with W352Y, W352H, W352A, and W352R mutations. The average of three experiments with standard errors is shown.

9-1-1 and indirect activation by 9-1-1 via Dpb11 contribute to checkpoint function in G2/M. We measured a stronger damage sensitivity phenotype in the complex *ddc1-2W2A,T602A* mutant compared with the pathway-specific mutants, i.e., *ddc1-2W2A* and *ddc1-T602A* (Figure 4C).

Mec1 Is Activated by a Small Peptide that Fuses the Two Conserved Motifs

The two motifs in Ddc1 that we identified as being essential for robust Mec1 activation are separated by a large region of unstructured protein that shows little or no sequence conservation, even in the closely related *Saccharomycetales* order (Figure 2A). The distance between the two motifs also varies widely, from 87 aa in *C. albicans* to 188 aa in *S. cerevisiae*. Thus, we tested whether the ability to activate Mec1 is solely embedded in the two essential motifs that we have identified. A 30-mer peptide was designed that contains the β strand-turn-β strand motif from the PCNA-like domain fused to the WG motif (with surrounding amino acids) from the unstructured tail. Remarkably, this small peptide showed robust activation of Mec1 kinase activity (Figure 5A). Activation is sensitive to increasing salt in the assay, as shown before for the full-length Ddc1 subunit (Majka et al., 2006b). Most significantly, W → A mutation of either the N-proximal or -distal tryptophan residue completely abrogates the capacity of the mutant peptide to activate Mec1 (Figure 5B). The essential W352 residue is Y271 in *S. pombe* Rad9 and H239 in human and *X. laevis* Rad9 (Figure S4). Peptides containing tyrosine or histidine in the proximal motif also activate Mec1, albeit with reduced efficiency. In contrast, a peptide with arginine at that position is completely inactive (Figure 5C). In human, the H239R mutation is associated

with an increased occurrence of lung adenocarcinomas (Maniwa et al., 2006).

DISCUSSION

Our comprehensive analysis of the Ddc1 subunit of yeast 9-1-1 has identified three distinct functions for this protein: (1) its function as a subunit of 9-1-1, (2) activation of Mec1 protein kinase activity, and (3) binding of its phosphorylated form to Dpb11, thereby promoting indirect activation of Mec1 kinase activity. The latter two functions require Ddc1 to be a functional subunit of 9-1-1, which can be loaded onto partially double-stranded DNA by its loader Rad24-RFC. This follows from the observation that the *ddc1-ILM360-362AAA* mutant, which is proficient for activating Mec1 in vitro but cannot form a 9-1-1 clamp, has a phenotype similar to the *ddc1Δ* mutant (Figure S5D). Eliminating from Ddc1 the ability to activate Mec1 and to bind Dpb11 results in a less-severe damage sensitivity phenotype than that of a *DDC1* deletion, suggesting that the clamp itself has additional genome stability functions that are unrelated to checkpoint function (Figure 4C). The 9-1-1 clamp has been shown to interact with the nucleotide excision repair, base excision repair, and translesion synthesis machineries; however, the relevance of these interactions still requires investigation (reviewed in Navadgi-Patil and Burgers, 2009).

A Bipartite Activation Motif in Ddc1 for Activation of Mec1 Kinase

Our studies with a Ddc1 peptide comprising both required activation motifs indicates that the two tryptophans are essential determinants for activity, because a mutation of either tryptophan to alanine results in a complete loss of Mec1 activation (Figure 5B). *Xenopus* ATR activation by xTopBP1 is also eliminated in an xTopBP1-W1138R mutant, underscoring the importance of aromatic amino acids in the activation of Mec1/ATR (Kumagai et al., 2006). While the 30-mer peptide shows robust activation of Mec1, it does require much higher peptide concentrations than the full-length Ddc1 subunit, suggesting that additional regions of Ddc1 contribute to binding Mec1 with high affinity.

The strong sequence conservation in the PCNA homology region of Ddc1 with that of other Rad9/Ddc1 subunits suggests that both structure and function are conserved (Figures 6 and S4). Interestingly, a projection of the essential Ddc1-W352 residue onto the crystal structure of human 9-1-1 shows that the analogous H239 residue of human Rad9 is solvent-exposed near the outer rim of the donut, allowing, in principle, for an interaction with human ATR (Figure 6A) (Doré et al., 2009; Sohn and Cho, 2009). The adjacent residues, Ile238 and Phe240, are buried inside the protein and are required for structural integrity (Figure 6B), and indeed, mutation of the analogous Ddc1 residues to alanine leads to misfolding and loss of subunit-subunit interactions (Figure S5B). The C-terminal tail of Rad9 is missing from both published 9-1-1 structures. This tail is expected to exit the ring structure close to the hRad9-H239 residue (Figure 6B). Currently, it is not yet evident on which side of the donut the clamp loader binds, and therefore, the orientation of the clamp on the DNA also remains to be established. However, since H239 is near the outer rim of the donut, either orientation of the clamp could conceivably permit interactions with Mec1/ATR.

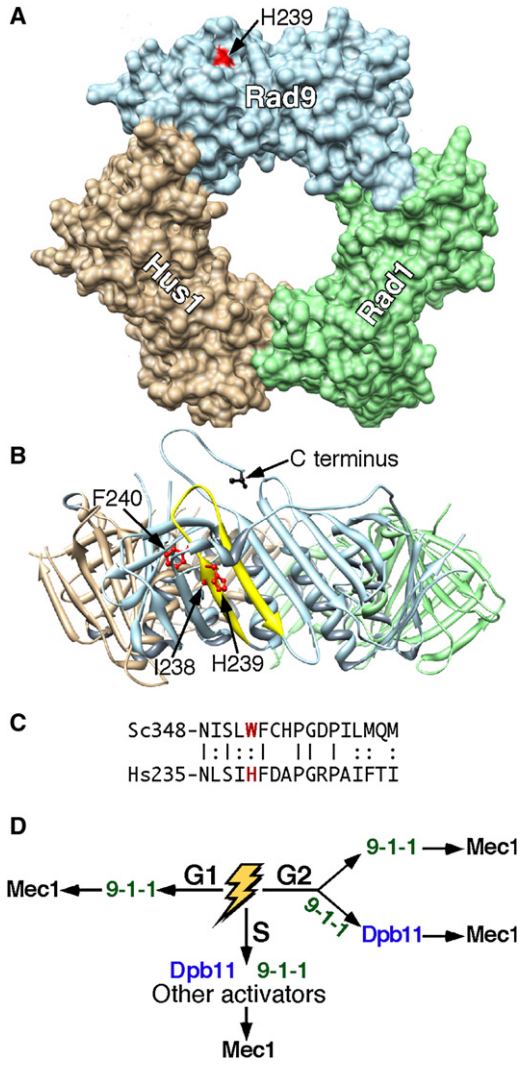

Figure 6. Role of 9-1-1 in Two Distinct Checkpoint Pathways

(A) Surface representation of the 9-1-1 crystal structure (Doré et al., 2009); head-on view with I238, H239, and F240 in red. Note that only H239 is surface exposed. The Rad9 C terminus is in back of the donut. The Chimera molecular viewer was used (Pettersen et al., 2004).

(B) Ribbon representation after a 90° x axis rotation. The Rad9 (aa 235–252) β strand-loop-β strand is in yellow, with I238, H239, and F240 as stick models in red. The C-terminal aa 273 of truncated Rad9 is shown in black.

(C) Alignment of the β strand-loop-β strand of human Rad9 with yeast Ddc1.

(D) Model for the participation of 9-1-1 in two pathways, depending on the phase of the cell cycle.

Mec1/ATR Activation by the 9-1-1 Clamp and by Dpb11/TopBP1

Our studies with *S. cerevisiae* checkpoint factors have established that both 9-1-1 and Dpb11 can independently activate Mec1 kinase activity in vitro. The analysis in this paper shows that, in the G1 phase of the cell cycle, 9-1-1 can activate Mec1

in the absence of functional Dpb11. On the other hand, during G2/M, either 9-1-1 or Dpb11 can activate Mec1; however, the latter mechanism requires the participation of 9-1-1 as a recruitment factor rather than as a Mec1 activator. This follows from the observation that the activation-defective *ddc1-2w2A* mutant is still functional in the Dpb11-dependent pathway, whereas the recruitment-defective *ddc1-T602A* mutant abrogates this pathway. Both functions of 9-1-1 are required for full checkpoint activation in G2 (Figure 4A). Our studies agree with a previous study showing dependence on the phosphorylation of Ddc1 for a full G2 checkpoint (Puddu et al., 2008). From our studies, we cannot conclude whether both pathways function in G2/M in mounting a checkpoint response to all types of DNA damage, i.e., are partially redundant, or whether the particular DNA structure onto which 9-1-1 is loaded dictates which pathway is used, direct activation of Mec1 by 9-1-1 or activation via Dpb11.

Our genetic studies have been confined to the G1 and G2 phases of the cell cycle because DNA damage response pathways are better defined than those during S phase. While the G1 and G2 responses are completely dependent on 9-1-1, Mec1 activation during S phase still proceeds in a *ddc1Δ* strain. A somewhat reduced but still substantial degree of Rad53 phosphorylation is observed in a *ddc1Δ dpb11-1* double mutant subjected to DNA damage or to the replication inhibitor hydroxyurea (Figure S2C). This phosphorylation of Rad53 proceeds through Mec1 (Paciotti et al., 2001). Therefore, it is highly likely that additional S phase-specific activator(s) of Mec1 exist in *S. cerevisiae*.

So far, evidence that 9-1-1 clamps from other organisms can directly activate ATR is still lacking. Information regarding the relative roles of 9-1-1 and Cut5/TopBP1 come from genetic studies in *S. pombe* and human and from *Xenopus* extract studies. These studies indicate an interdependence of 9-1-1 and Cut5/TopBP1 for efficient checkpoint function and have shown that phosphorylation of Rad9 for recruitment of Cut5/TopBP1 is an essential step in this pathway (Delacroix et al., 2007; Furuya et al., 2004; Marchetti et al., 2002). One possible explanation for resolving the discrepancy between checkpoint pathway models between *S. cerevisiae* and the other model organisms lies in the realization that only in the *S. cerevisiae* G1 phase is the checkpoint completely dependent on 9-1-1 and not on Dpb11. This pathway is strongly coupled to NER of the damage imposed upon the cell (Giannattasio et al., 2004). G1 checkpoints have received much less attention in other model organisms, and while coupling of NER to the checkpoint has been studied in human cells, the relative requirements of TopBP1 and 9-1-1 still remain to be established (Marini et al., 2006). Unfortunately, *S. pombe*, which has proven to be such an excellent model for checkpoint studies, has not been subjected to complementary biochemical studies, and therefore, the question whether 9-1-1 can directly activate *S. pombe* Rad3 (Mec1/ATR) remains open.

A Polymorphism at Human H239 Is Associated with Lung Adenocarcinoma

A recent report showed that 16% of patients with lung adenocarcinoma were heterozygous for a H239R mutation in the human RAD9A gene (Maniwa et al., 2006). The study suggests that if there is a causal relationship between the H239R mutation and the occurrence of adenocarcinomas, the H239R mutation may display a dominant-negative phenotype, because cancer formation is not associated with loss of heterozygosity at RAD9. These observations can be explained by our current model for 9-1-1 function in *S. cerevisiae*. Mutation of W352 of Ddc1, which is homologous to hRad9-H239, results in a loss of Mec1 activation, but not in a defect in clamp structure or loading. Our prediction is that the human Rad9-H239R mutant subunit, while still able to form a clamp and load onto DNA, would be inactive for ATR activation, thereby explaining the partial dominance of this mutation. While we have not been able to elicit activation of yeast Mec1 by the human Rad9 protein (data not shown), we note that in our peptide activation studies, substitution of the essential W352 residue by histidine (reflecting H239) still yields a bioactive peptide, whereas substitution with arginine (reflecting the H239A adenocarcinoma mutation) results in complete loss of activity (Figure 5C). Our data suggest that human Rad9 is involved in the activation of ATR under some conditions, and this activation is compromised in the Rad9-H239R mutant, leading to genome instability and cancer progression.

EXPERIMENTAL PROCEDURES

Strains, Plasmids, and Proteins

All yeast strains, plasmids, and protein complexes used in this study are described in the Supplemental Data.

Mec1 Activation Assays

Two distinct Mec1 activation assays were used.

Complete Assay (Dependent on 9-1-1, Rad24-RFC, and DNA)

Single-stranded Bluescript SKII$^+$ DNA was primed with ten 28-mer primers spaced approximately equally around the 2.96 kb ssDNA circle. Phosphorylation assays (20 μl) contained 25 mM HEPES 7.8, 8 mM $MgAc_2$, 1 mM DTT, 100 μg/ml BSA, 50 μM [γ-^{32}P]ATP, 125 mM NaCl, 2.5 nM deca-primed ssSKII DNA, and 125 nM Rad53-kd. The DNA was coated with 200 nM RPA on ice, 30 nM Rad24-RFC and the indicated concentrations of wild-type or mutant 9-1-1 were added, and the reaction was incubated at 30°C for 1 min to allow loading of 9-1-1. The reaction was then initiated with 5 nM Mec1 kinase. After 10 min, the reaction was terminated by addition of 5 μl 5× SDS-PAGE loading buffer. The phosphorylated polypeptides were separated using SDS-PAGE; the gel was dried and analyzed using phosphorimaging. For quantification purposes, a phosphate standard curve was generated by spotting serial dilutions of the assay mix onto the dried gel.

Low-NaCl Bypass Assay (Dependent on Ddc1)

Buffer conditions were the same; however, the assay contained only 40 mM NaCl and no DNA, RPA, and Rad24-RFC. Analysis was as described above. This assay was used for the study of activation of Mec1 by peptides. Reactions contained either peptide dilution buffer or peptide. Control studies showed that peptide dilution buffer did not significantly inhibit Mec1 activation by Ddc1.

Analysis of Checkpoint Clamp Loading onto DNA

Clamp loading assays and separation of DNA-bound 9-1-1 from free 9-1-1 by Bio-Gel A 15 m size exclusion chromatography were performed as described (Majka and Burgers, 2003). The DNA-protein fractions were pooled together, proteins were separated by 10% SDS-PAGE, and (mutant) Ddc1 was detected by western analysis with a rabbit antibody to Ddc1.

Western Analysis of Rad53 Phosphorylation

Cells were grown in 5 ml of selective media to OD_{660} = 0.5. They were then arrested in G1 phase by α factor (20 μg/ml for 2 hr) or in G2 with nocodazole (20 μg/ml for 3 hr) and treated with 4NQO (2 μg/ml) or methylmethane sulfonate (0.1%) for 30 min at 30°C. After exposure to the indicated DNA damaging

agents, protein extracts were prepared by trichloroacetic acid (TCA) precipitation. The Rad53 YC-19 antibody (Santa Cruz Biotechnology; Santa Cruz, CA) was used at a 1000-fold dilution in TBS containing 5% milk and 0.1% Tween 20. Alkaline phosphatase-conjugated anti-goat secondary antibody (Sigma) was used at a 5000-fold dilution in TBS containing 5% milk and 0.1% Tween 20. Rad53 was detected using an ECF substrate (GE Healthcare; Piscataway, NJ) and scanned using a Typhoon scanner (GE Healthcare).

DNA Damage Sensitivity Assays

Strains were transformed either with empty vector or with plasmids (pBL760 and pBL782 series) encoding wild-type or mutant *DDC1*. The transformants were grown up to log phase in SC media lacking tryptophan. Serial dilutions of cells were spotted on YPD plates or YPD plates containing camptothecin. For UV irradiation, YPD plates were exposed to the indicated dose of UV_{254}. The plates were incubated at 30°C for 2 days and photographed. To quantify the cell survival in response to UV, cells were spread on YPD plates and exposed to UV light. After incubation at 30°C for 2 days, the colonies were counted, and cell survival was plotted as a function of UV dose.

SUPPLEMENTAL DATA

Supplemental Data include Supplemental Experimental Procedures, Supplemental References, three tables, and seven figures and can be found online at http://www.cell.com/molecular-cell/supplemental/S1097-2765(09)00779-5.

ACKNOWLEDGMENTS

We thank Jurek Majka for help and advice during the initial stages of this work, John Majors for critical discussions, and Carrie Stith for expert technical assistance. This work was supported in part by NIH grants GM32431 and GM083970.

Received: July 30, 2009
Revised: September 11, 2009
Accepted: September 23, 2009
Published: December 10, 2009

REFERENCES

Araki, H., Leem, S.H., Phongdara, A., and Sugino, A. (1995). Dpb11, which interacts with DNA polymerase II(epsilon) in Saccharomyces cerevisiae, has a dual role in S-phase progression and at a cell cycle checkpoint. Proc. Natl. Acad. Sci. USA *92*, 11791–11795.

Bakkenist, C.J., and Kastan, M.B. (2004). Initiating cellular stress responses. Cell *118*, 9–17.

Bonilla, C.Y., Melo, J.A., and Toczyski, D.P. (2008). Colocalization of sensors is sufficient to activate the DNA damage checkpoint in the absence of damage. Mol. Cell *30*, 267–276.

Choi, J.H., Lindsey-Boltz, L.A., and Sancar, A. (2007). Reconstitution of a human ATR-mediated checkpoint response to damaged DNA. Proc. Natl. Acad. Sci. USA *104*, 13301–13306.

Delacroix, S., Wagner, J.M., Kobayashi, M., Yamamoto, K., and Karnitz, L.M. (2007). The Rad9-Hus1-Rad1 (9-1-1) clamp activates checkpoint signaling via TopBP1. Genes Dev. *21*, 1472–1477.

Doré, A.S., Kilkenny, M.L., Rzechorzek, N.J., and Pearl, L.H. (2009). Crystal structure of the rad9-rad1-hus1 DNA damage checkpoint complex—implications for clamp loading and regulation. Mol. Cell *34*, 735–745.

Frei, C., and Gasser, S.M. (2000). The yeast Sgs1p helicase acts upstream of Rad53p in the DNA replication checkpoint and colocalizes with Rad53p in S-phase-specific foci. Genes Dev. *14*, 81–96.

Furuya, K., Poitelea, M., Guo, L., Caspari, T., and Carr, A.M. (2004). Chk1 activation requires Rad9 S/TQ-site phosphorylation to promote association with C-terminal BRCT domains of Rad4TOPBP1. Genes Dev. *18*, 1154–1164.

Giannattasio, M., Sommariva, E., Vercillo, R., Lippi-Boncambi, F., Liberi, G., Foiani, M., Plevani, P., and Muzi-Falconi, M. (2002). A dominant-negative MEC3 mutant uncovers new functions for the Rad17 complex and Tel1. Proc. Natl. Acad. Sci. USA *99*, 12997–13002.

Giannattasio, M., Lazzaro, F., Longhese, M.P., Plevani, P., and Muzi-Falconi, M. (2004). Physical and functional interactions between nucleotide excision repair and DNA damage checkpoint. EMBO J. *23*, 429–438.

Green, C.M., Erdjument-Bromage, H., Tempst, P., and Lowndes, N.F. (2000). A novel Rad24 checkpoint protein complex closely related to replication factor C. Curr. Biol. *10*, 39–42.

Harrison, J.C., and Haber, J.E. (2006). Surviving the breakup: the DNA damage checkpoint. Annu. Rev. Genet. *40*, 209–235.

Kumagai, A., Lee, J., Yoo, H.Y., and Dunphy, W.G. (2006). TopBP1 activates the ATR-ATRIP complex. Cell *124*, 943–955.

Longhese, M.P., Paciotti, V., Fraschini, R., Zaccarini, R., Plevani, P., and Lucchini, G. (1997). The novel DNA damage checkpoint protein ddc1p is phosphorylated periodically during the cell cycle and in response to DNA damage in budding yeast. EMBO J. *16*, 5216–5226.

MacDougall, C.A., Byun, T.S., Van, C., Yee, M.C., and Cimprich, K.A. (2007). The structural determinants of checkpoint activation. Genes Dev. *21*, 898–903.

Majka, J., and Burgers, P.M. (2003). Yeast Rad17/Mec3/Ddc1: a sliding clamp for the DNA damage checkpoint. Proc. Natl. Acad. Sci. USA *100*, 2249–2254.

Majka, J., Binz, S.K., Wold, M.S., and Burgers, P.M. (2006a). Replication protein A directs loading of the DNA damage checkpoint clamp to 5′-DNA junctions. J. Biol. Chem. *281*, 27855–27861.

Majka, J., Niedziela-Majka, A., and Burgers, P.M. (2006b). The checkpoint clamp activates Mec1 kinase during initiation of the DNA damage checkpoint. Mol. Cell *24*, 891–901.

Maniwa, Y., Yoshimura, M., Bermudez, V.P., Okada, K., Kanomata, N., Ohbayashi, C., Nishimura, Y., Hayashi, Y., Hurwitz, J., and Okita, Y. (2006). His239Arg SNP of HRAD9 is associated with lung adenocarcinoma. Cancer *106*, 1117–1122.

Marchetti, M.A., Kumar, S., Hartsuiker, E., Maftahi, M., Carr, A.M., Freyer, G.A., Burhans, W.C., and Huberman, J.A. (2002). A single unbranched S-phase DNA damage and replication fork blockage checkpoint pathway. Proc. Natl. Acad. Sci. USA *99*, 7472–7477.

Marini, F., Nardo, T., Giannattasio, M., Minuzzo, M., Stefanini, M., Plevani, P., and Muzi Falconi, M. (2006). DNA nucleotide excision repair-dependent signaling to checkpoint activation. Proc. Natl. Acad. Sci. USA *103*, 17325–17330.

Mordes, D.A., Nam, E.A., and Cortez, D. (2008). Dpb11 activates the Mec1-Ddc2 complex. Proc. Natl. Acad. Sci. USA *105*, 18730–18734.

Navadgi-Patil, V.M., and Burgers, P.M. (2008). Yeast DNA replication protein Dpb11 activates the Mec1/ATR checkpoint kinase. J. Biol. Chem. *283*, 35853–35859.

Navadgi-Patil, V.M., and Burgers, P.M. (2009). A tale of two tails: activation of DNA damage checkpoint kinase Mec1/ATR by the 9-1-1 clamp and by Dpb11/TopBP1. DNA Repair (Amst.) *8*, 996–1003.

Paciotti, V., Clerici, M., Scotti, M., Lucchini, G., and Longhese, M.P. (2001). Characterization of mec1 kinase-deficient mutants and of new hypomorphic mec1 alleles impairing subsets of the DNA damage response pathway. Mol. Cell. Biol. *21*, 3913–3925.

Parrilla-Castellar, E.R., Arlander, S.J., and Karnitz, L. (2004). Dial 9-1-1 for DNA damage: the Rad9-Hus1-Rad1 (9-1-1) clamp complex. DNA Repair (Amst.) *3*, 1009–1014.

Pellicioli, A., Lucca, C., Liberi, G., Marini, F., Lopes, M., Plevani, P., Romano, A., Di Fiore, P.P., and Foiani, M. (1999). Activation of Rad53 kinase in response to DNA damage and its effect in modulating phosphorylation of the lagging strand DNA polymerase. EMBO J. *18*, 6561–6572.

Pettersen, E.F., Goddard, T.D., Huang, C.C., Couch, G.S., Greenblatt, D.M., Meng, E.C., and Ferrin, T.E. (2004). UCSF Chimera—a visualization system for exploratory research and analysis. J. Comput. Chem. *25*, 1605–1612.

Puddu, F., Granata, M., Di Nola, L., Balestrini, A., Piergiovanni, G., Lazzaro, F., Giannattasio, M., Plevani, P., and Muzi-Falconi, M. (2008). Phosphorylation of the budding yeast 9-1-1 complex is required for Dpb11 function in the full activation of the UV-induced DNA damage checkpoint. Mol. Cell. Biol. *28*, 4782–4793.

Rouse, J., and Jackson, S.P. (2002). Lcd1p recruits Mec1p to DNA lesions in vitro and in vivo. Mol. Cell *9*, 857–869.

Sohn, S.Y., and Cho, Y. (2009). Crystal structure of the human rad9-hus1-rad1 clamp. J. Mol. Biol. *390*, 490–502.

Tercero, J.A., and Diffley, J.F. (2001). Regulation of DNA replication fork progression through damaged DNA by the Mec1/Rad53 checkpoint. Nature *412*, 553–557.

Wang, H., and Elledge, S.J. (2002). Genetic and physical interactions between DPB11 and DDC1 in the yeast DNA damage response pathway. Genetics *160*, 1295–1304.

Zou, L., and Elledge, S.J. (2003). Sensing DNA damage through ATRIP recognition of RPA-ssDNA complexes. Science *300*, 1542–1548.

Supplemental Data
Molecular Cell, *Volume 36*

The Unstructured C-Terminal Tail of the 9-1-1 Clamp Subunit Ddc1 Activates Mec1/ATR via Two Distinct Mechanisms

Vasundhara M. Navadgi-Patil and Peter M. Burgers

SUPPLEMENTAL EXPERIMENTAL PROCEDURES

S. cerevisiae strains were obtained from S. Elledge (Harvard Medical School) and are derived from Y300 (MAT**a** *ade2-1 trp1-1 ura3-1* leu2-3 *his3-11*); Y1135 (*ddc1Δ::HIS3*), Y1185 (*dpb11-1*), and Y1189 (*dpb11-1 ddc1Δ::HIS3*).

Plasmids and DNA Substrates

Standard methodologies were used to generate the plasmids containing *DDC1* mutants. Plasmids are available from authors upon request. *DDC1* was cloned under control of its native promoter into the yeast centromeric plasmid pRS314 (Sikorski and Hieter, 1989), to generate pBL785 (bluescript *ARS CEN TRP1 DDC1*). pBL760 (Ddc1) and pBL775 (GST-Ddc1) (2 μM origin, *TRP*, *GAL1-10* promoter for galactose inducible expression) are described in (Majka and Burgers, 2003; Majka and Burgers, 2005)**.** Point mutations were generated by site directed mutagenesis (Stratagene). DNA coding for Ddc1 truncated proteins were PCR amplified and cloned in *E. coli* expression vector pGEX-6p1 (GE Healthcare) to generate plasmids in the pBL783 series.

Peptides and Checkpoint Proteins

All peptides were from Genscript (Piscataway, NJ) and had purity higher than 70%. The peptides were desalted and dissolved in appropriate buffers, containing up to 5% dimethyl formamide if necessary, to a final concentration of 1 mM. Rad24-RFC, Rad53-kd, Mec1/Ddc2, and RPA were purified as

described earlier (Majka and Burgers, 2003; Majka et al., 2006). To purify the checkpoint clamp, pBL775 expressing GST-*DDC1* and pBL763 expressing *RAD17* and *MEC3* (all genes were on multicopy vectors under control of the galactose-inducible GAL1-10 promoter) were co transformed into yeast strain FM113 (MAT**a** *ura3-52 trp1-289 leu2-3 112 prb1-1122 prc1-407 pep4-3*). Media have been described before (Bylund et al., 2006). Cells were grown in 6-liter SCGL media lacking uracil and tryptophan, till late log phase and induced with 2% galactose in YPGL media for 5 hr. Cells were centrifuged and stored as popcorn made in liquid nitrogen. 50 g of yeast cells were blended in dry ice with 50 ml of 2x buffer A containing 300 mM KCl (buffer A: 50 mM Hepes, pH 7.5, 10% glycerol, 1 mM DTT, 0.01% Nonidet P-40, 1mM EDTA, 1mM EGTA) and protease inhibitors (1mM PMSF, 2 µM pepstatin A, 2 µM leupeptin, 10 mM $NaHSO_3$, 1 mM benzamidine) followed by polyamine P precipitation and centrifugation at 16000 rpm for 1 hr as described before (Bylund et al., 2006). The supernatant was allowed to batch bind to 1 ml glutathione-sepharose for 2 hr, and the beads spun down and loaded in a column. The column was washed serially with 50 ml of buffer A containing 100 mM KCl (A_{100}), 25 ml of buffer A_{100} with 1 mM ATP and 1 mM $MgCl_2$ and finally with 50 ml of buffer A_{100} without protease inhibitors. GST- Ddc1/Rad17/Mec3 was eluted with 20 mM glutathione in buffer A_{100} and digested with 20 units of 3C protease overnight at 4^oC. GST cleaved clamp was loaded onto a 1 ml heparin column (GE Healthcare) in buffer A_{100}. GST and 3C protease do not bind heparin and are retained in the flow through. The column was washed with 10 ml of A_{100}. Excess Ddc1 (which is not part of the clamp) eluted early from the column at 180 mM KCl, and the heterotrimeric clamp was eluted with A_{500}. Other clamps with various Ddc1 mutations were grown and purified in a similar way.

To purify individual Ddc1 truncated proteins, the pBL783 series of plasmids was transformed in *E.coli* BL21 (DE3) cells and proteins induced with 1 mM IPTG for 4 hr. Cells were lysed in buffer A_{500}, sonicated and centrifuged at 16000 rpm for 1 hr. Proteins were purified sequentially on a glutathione-affinity column and heparin-ion exchange column with purification conditions analogous to that of the clamp.

In Situ Autophosphorylation Assay

Cells were arrested in G1 phase by alpha factor (20 μg/ml) and treated with 4NQO (2 μg/ml) for 30 min at 30^{o}C. Proteins extracts were prepared by TCA precipitation, and Rad53 *in situ* autophosphorylation assays were essentially performed as described (Pellicioli et al., 1999). Briefly, extracts were separated by 8% SDS/PAGE, followed by electrophoretic transfer to nitocellulose membrane. Proteins on the membrane were renatured, and the blot incubated with carrier-free [γ-^{32}P]-ATP in buffer. After washes, the blot was analyzed on a phosphorimager.

Supplemental References

Bylund, G.O., Majka, J., and Burgers, P.M. (2006). Overproduction and purification of RFC-related clamp loaders and PCNA-related clamps from Saccharomyces cerevisiae. Methods Enzymol *409*, 1-11.

Majka, J., and Burgers, P.M. (2003). Yeast Rad17/Mec3/Ddc1: a sliding clamp for the DNA damage checkpoint. Proc. Natl. Acad. Sci. USA *100*, 2249-2254.

Majka, J., and Burgers, P.M. (2005). Function of Rad17/Mec3/Ddc1 and its partial complexes in the DNA damage checkpoint. DNA Repair (Amst) *4*, 1189-1194.

Majka, J., Niedziela-Majka, A., and Burgers, P.M. (2006). The checkpoint clamp activates Mec1 kinase during initiation of the DNA damage checkpoint. Mol Cell *24*, 891-901.

Pellicioli, A., Lucca, C., Liberi, G., Marini, F., Lopes, M., Plevani, P., Romano, A., Di Fiore, P.P., and Foiani, M. (1999). Activation of Rad53 kinase in response to DNA damage and its effect in modulating phosphorylation of the lagging strand DNA polymerase. EMBO Journal. *18*, 6561-6572.

Sikorski, R.S., and Hieter, P. (1989). A system of Shuttle Vectors and Yeast Host Strains Designed for Efficient Manipulation of DNA in *Saccharomyces cerevisiae*. Genetics *122*, 19-27.

Table S1. Plasmids Expressing *DDC1* (and Mutants) without Tag

Plasmid name	Ddc1 residues	Mutations
pBL760	1-612 aa	-
pBL760-1	1-612 aa	W544A
pBL760-2	1-612 aa	ILM360AAA
pBL760-3	1-612 aa	LWF351AAA
pBL760-8	1-612 aa	T602A
pBL760-20	1-612 aa	T342A ,S469A ,T529A ,S580A,T602A
pBL760-39	1-612 aa	W352A
pBL760-40	1-612 aa	W352A, W544A
pBL760-41	1-612 aa	W352A, T602A
pBL760-42	1-612 aa	W544A, T602A
pBL760-43	1-612 aa	W352A, W544A, T602A
pBL782	1-404 aa	-
pBL785	1-612 aa	-
pBL785-1	1-612 aa	T602A
pBL785-2	1-612 aa	W352A, W544A
pBL785-3	1-612 aa	W352A, W544A, T602A

Table S2. Plasmids Expressing *DDC1* (and Mutants) with GST Tag

pBL775	1-612 aa	-
pBL775-1	1-404 aa	
pBL775-2	1-508 aa	
pBL775-3	1-562 aa	
pBL775-4	1-612 aa	W544A
pBL775-6	1-612 aa	ILM360AAA
pBL775-7	1-612 aa	LWF351AAA
pBL775-12	1-612 aa	T602A
pBL775-5A	1-612 aa	T342A ,S469A ,T529A ,S580A,T602A
pBL775-16	1-612 aa	W352A
pBL775-17	1-404 aa	W352A
pBL775-18	1-612 aa	W352A, W544A

Table S3. Plasmids Expressing Ddc1 Domains with GST Tag for Overproduction in *E. coli*

pBL name	Ddc1 residues	Mutation
pBL783-4	294-612 aa	-
pBL783-5	340-562 aa	-
pBL783-6	348-562 aa	-
pBL783-7	357-562 aa	-
pBL783-9	366-612 aa	-
pBL783-11	405-612 aa	-
pBL783-12	340-562 aa	ILM360AAA
pBL783-13	340-562 aa	LWF351AAA

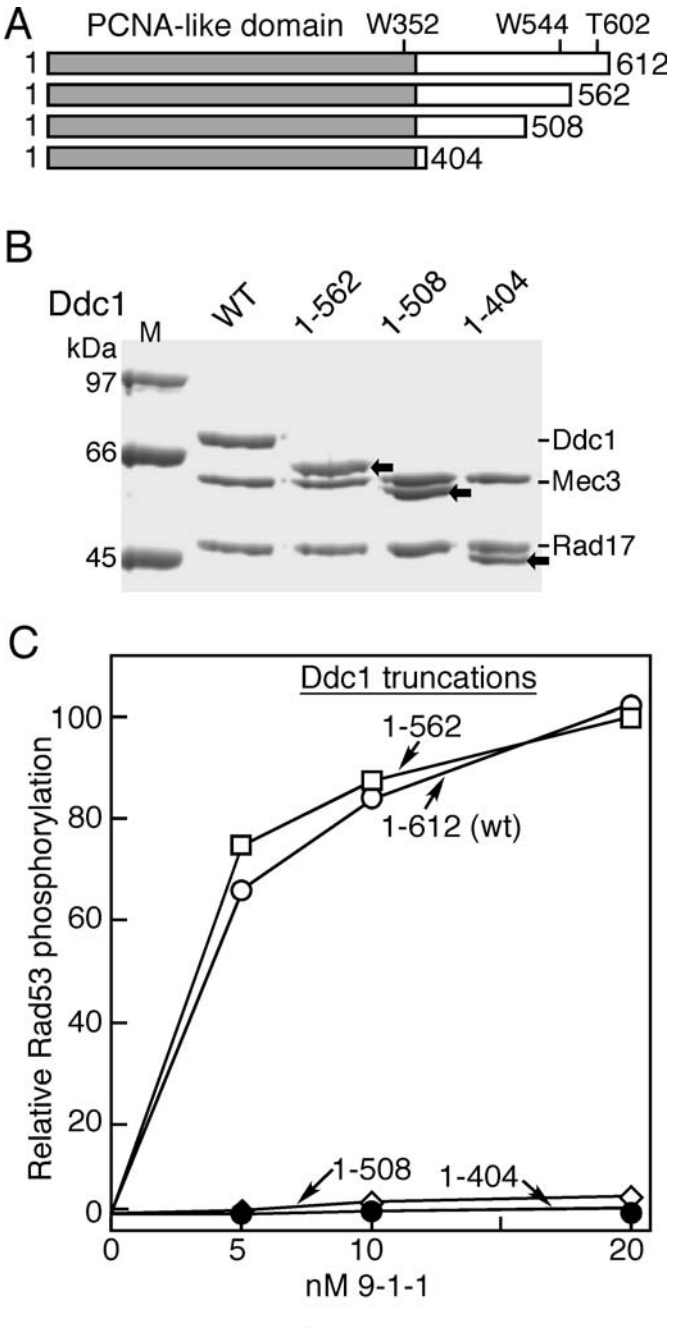

Figure S1. Analysis of 9-1-1 with Various C-Terminal Truncations of Ddc1

(A) Domain map of Ddc1 and its C-terminal mutants. The position of critical residues W352 and W544 involved in Mec1 activation are indicated.

(B) Coomassie-stained 10% SDS-PAGE gel showing the co-purification of Rad17 and Mec3 with wild-type Ddc1 and various Ddc1 C-terminal mutants when overexpressed in yeast. Arrows indicate the migration positions of Ddc1 and its mutants.

(C) Complete *in vitro* Mec1 phosphorylation assay was performed in the presence of varying amounts of the wild-type or mutant 9-1-1 clamp. Relative Rad53-kd phosphorylation was plotted against the concentration of the 9-1-1 clamp.

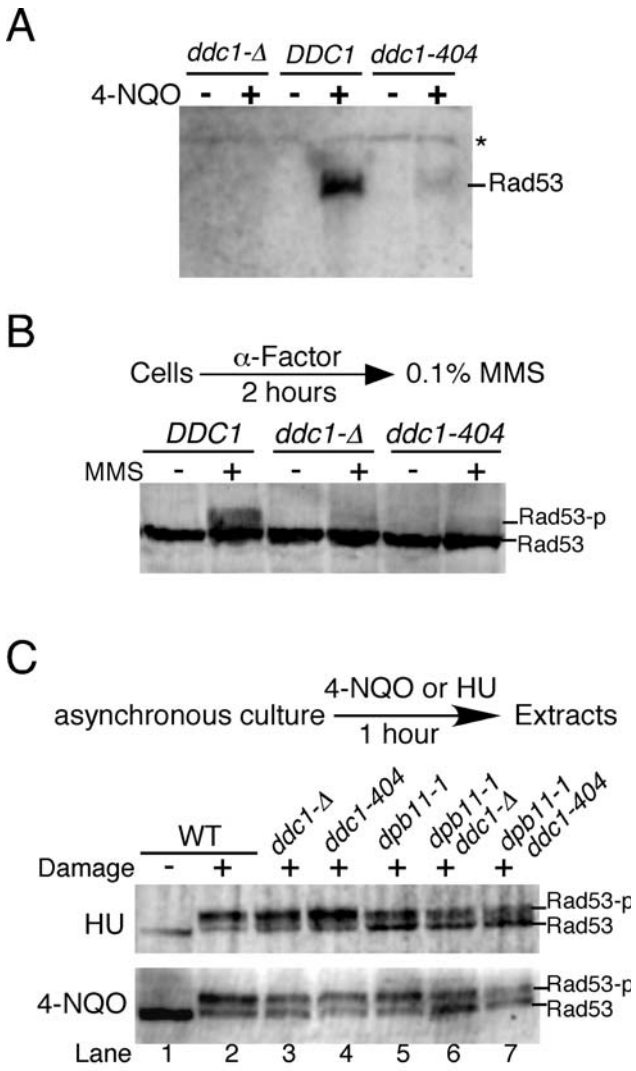

Figure S2. Analysis of Rad53 Phosphorylation in the *ddc1-404* and dpb11-1 Mutants

(A) G1-arrested cells were treated with or without 4NQO. *In situ* autophosphorylation assay was performed to detect activated Rad53. A nonspecific signal is indicated with an asterisk.

(B) Wild-type, *ddc1Δ* and *ddc1-404* cells were arrested in G1 phase and treated with 0.1% MMS for 30 min, as described in Methods. The hyperphosphorylated form of Rad53 is indicated as Rad53-p.

(C) Asynchronously growing *ddc1* or *dpb11-1* mutants cells at 25˚C were treated with or without 4NQO (2 µg/ml) or hydroxyurea (200 mM) for 1 hr. TCA extracts of these cells were subjected to a Western analysis with anti Rad53 antibody.

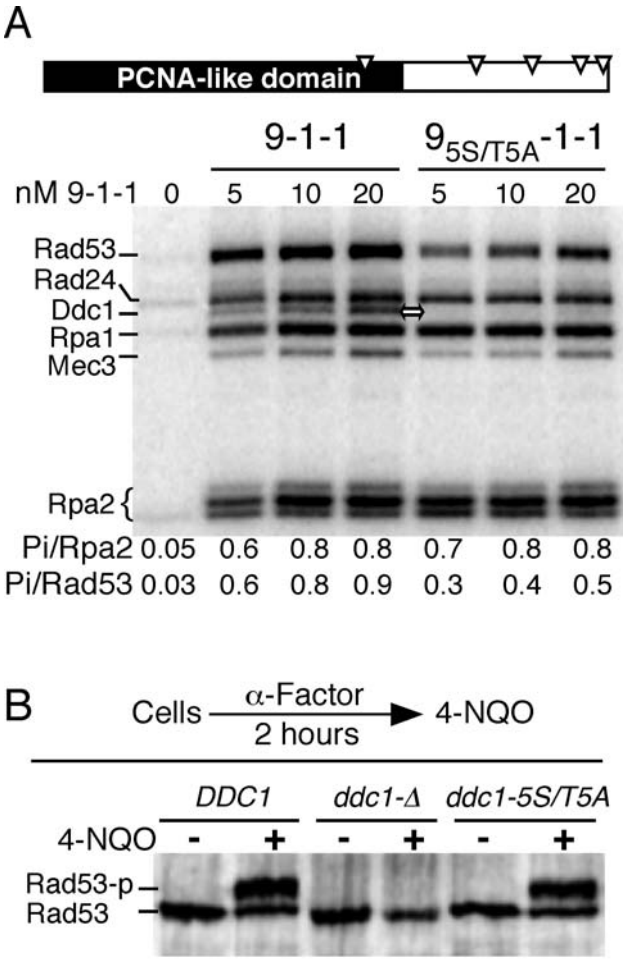

Figure S3. Ddc1 Phosphorylation Is Not Required to Activate Mec1

(A) Domain map of Ddc1 is shown. The open triangles indicate the five putative Mec1 phosphorylation sites (S/TQ) in Ddc1 (T342, S469, T529, S580, and T602). Indicated levels of wild-type or mutant 9-1-1 clamp were added to the complete Mec1 phosphorylation assay. Phosphorylated wild-type Ddc1 is indicated by an arrow. Note that Ddc1-5S/T5A mutant protein is not phosphorylated by Mec1. Quantification of phosphorylated Rpa2 and Rad53-kd is shown beneath the lanes.

(B) Western analysis of G1-arrested cells exposed to 4NQO for 30 min.

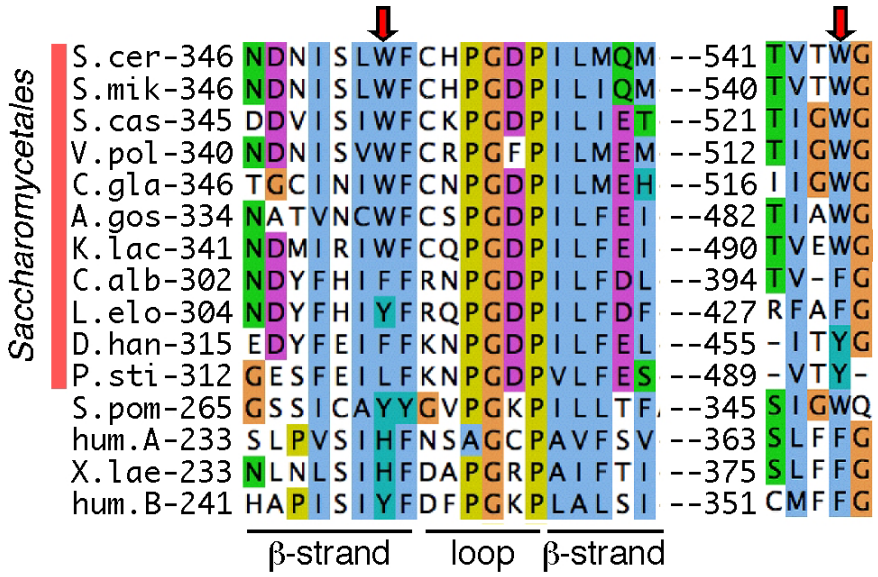

Figure S4. Multiple Sequence Alignment of the Ddc1 Motifs Involved in Mec1 Activation

Abreviations are S.cer, *Saccharomyces cerevisiae*; S.mik, *Saccharomyces mikatae*; S.cas, *Saccharomyces castela*; V.pol, *Vanderwaltozyma polyspora*; C.gla, *Candida glabrata*; A.gos, *Ashbya gossypii*; K.lac, *Kluyveromyces lactis*; C.alb, *Candida albicans*; L.elo, *Lodderomyces elongisporus*; D.han, *Debaryomyces hansenii*;P.sti, *Pichia stipitis*; S.pom, *Schizosaccharomyces pombe*; hum.A, human RAD9A; hum.B, human RAD9B; X.lae, *Xenopus laevis*. Species from the *Saccharomycetales* order are indicated.

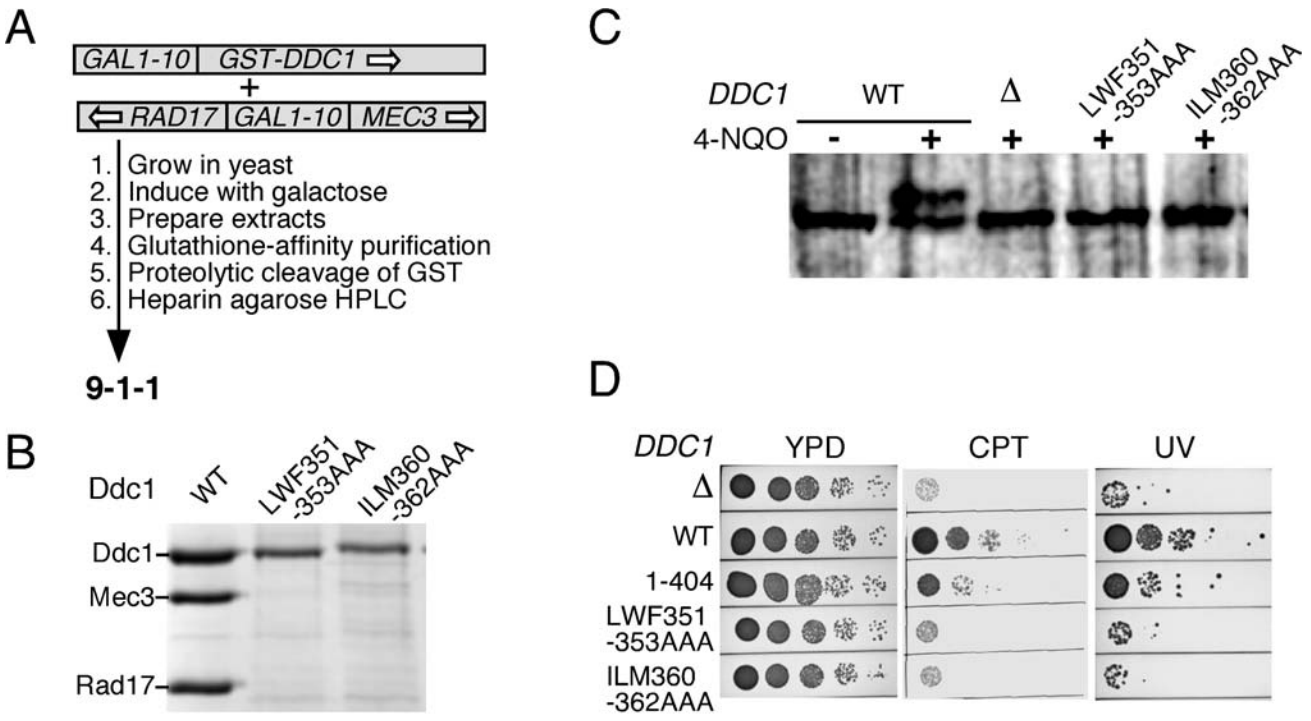

Figure S5. Analysis of Triple Mutants in β-Strands of Ddc1

(A) Schematic for overexpression and purification of the 9-1-1 complex.

(B) Coomassie stained 10 % SDS-PAGE gel showing that the indicated Ddc1 mutants are defective for interaction with Rad17 and Mec3. Lane 1, wild-type 9-1-1 clamp obtained from a 9-1-1 overexpression experiment with wild-type Ddc1; lane 2, 3 Ddc1-LWF351AAA and Ddc1-ILM360AAA, obtained from 9-1-1 overexpression experiments with the respective mutants of Ddc1.

(C) Wild-type or mutant cells were arrested in G1 phase and treated with 4NQO (2 µg/ml) for 15 min, as described in Experimental Procedures.

(D) Serial dilutions of wild-type and the indicated *ddc1* mutants were tested for sensitivity to camptothecin (10 µg/ml) and UV (50 J/m^2). The plates were incubated at 30°C for 2 days and photographed.

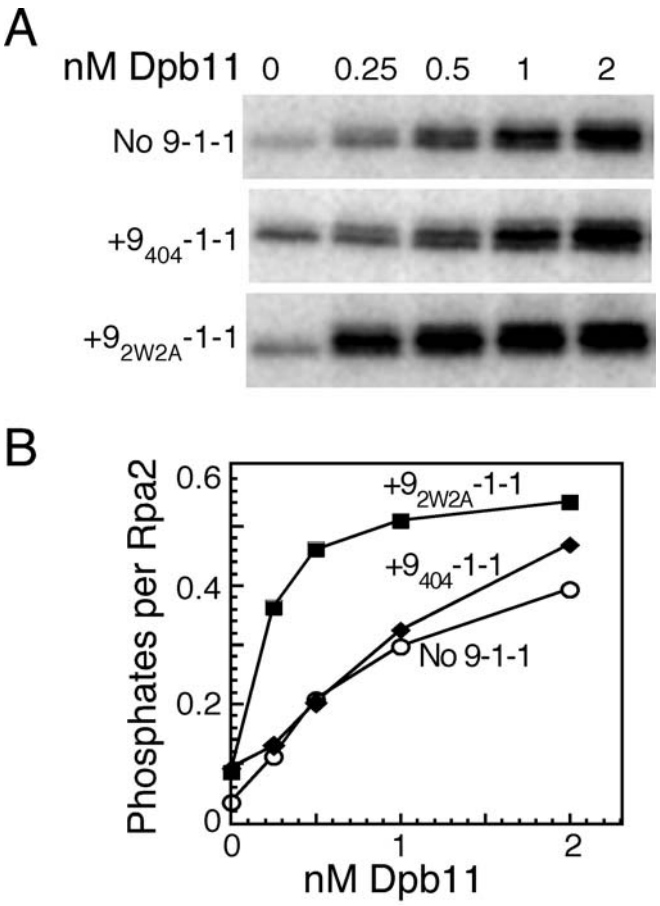

Figure S6.

(A) Complete Mec1 activation assay was performed with indicated amount of Dpb11 either in the absence of the checkpoint clamp or in the presence of the 20 nM 9_{2W2A}-1-1 or 9_{404}-1-1 clamps. RPA2 phosphorylation is shown. (B) Quantification of RPA2 phosphorylation by Mec1 from (A).

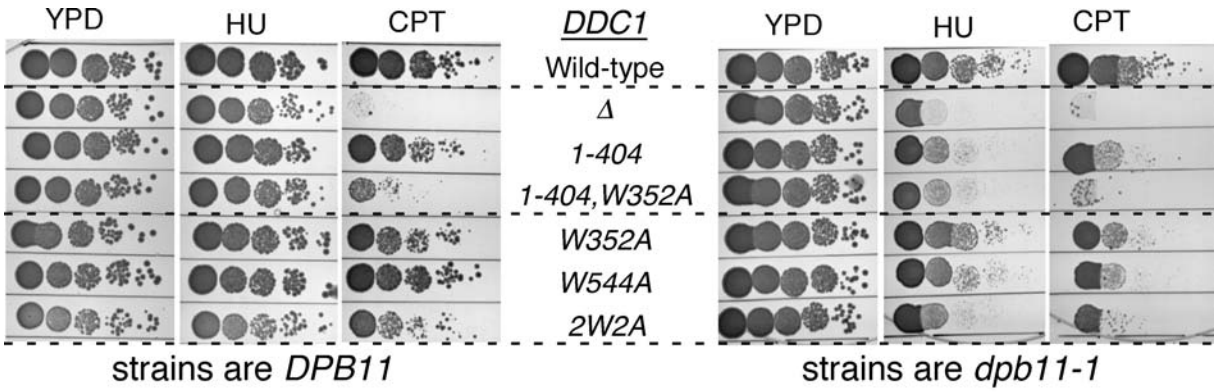

Figure S7.

Serial dilutions of wild-type and the indicated *ddc1* mutants in *DPB11* and *dpb11-1* background were tested for sensitivity to hydroxyurea and camptothecin. The plates were incubated at 23 ^{0}C for three days and photographed.